

Water in Hydrogels. 1. A Study of Water in Poly(*N*-vinyl-2-pyrrolidone/methyl methacrylate) Copolymer

Francis X. Quinn, Eithne Kampff, Gerard Smyth, and Vincent J. McBrierty*

Department of Pure and Applied Physics, Trinity College, Dublin 2, Ireland.
Received January 21, 1988; Revised Manuscript Received April 27, 1988

ABSTRACT: This paper seeks a clearer understanding of the role of water in hydrated polymers. Pulsed NMR relaxation data for the hydrated copolymer poly(*N*-vinyl-2-pyrrolidone/methyl methacrylate), P-(NVP/MMA), reveal that a significant part of the water is nonfreezable or bound in the sense that it becomes mobile, much like a glass, at ~ 170 K. Consideration of T_2 component intensities allows one to estimate the relative fractions of three distinguishably different types of water in P(NVP/MMA). The bound water can be resolved into a mobile component characterized by a long T_2 (type A) and a component of lower mobility that combines with plasticized polymer to form an intermediate T_2 (type B). In samples with water content in excess of ≈ 76 wt % there is also bulklike water that freezes in the vicinity of 273 K. Parallel DSC measurements predict a lower estimate for the amount of nonfreezable water which correlates rather well with the amount of type A water present. Intercomparison of NMR and DSC data is facilitated by a scheme that envisages five thermal equilibrium states in hydrated P(NVP/MMA). This study highlights the importance of taking the plasticized polymer contribution into account in estimating bound water by the NMR technique.

Introduction

The burgeoning literature on the role of water in natural and synthetic polymers attests to the scientific and commercial importance of these systems.¹⁻³ Substantial progress has been made in unraveling the inherent complexities of water/polymer interactions, with most attention focused upon water in natural polymers, particularly proteins and polypeptides, and in those synthetic polymers such as poly(2-hydroxyethyl methacrylate) (PHEMA) that are biologically compatible.

It is generally the case that water in polymers behaves abnormally in the sense that the sharp first-order phase transitions characteristic of bulk water are not observed in the usual manner. Stillinger⁴ has pointed out that modifications in water phase transitions result from finite size effects where the presence of boundaries and interfaces reduces the number of degrees of freedom and disrupts the natural order in the bulk phase. By the same token, clustering leads to supercooling due principally to the presence of fewer nucleating seeds in a cluster of limited size.

Binding sites in the polymer also play an important part. Rowland and Kuntz⁵ recognize an emerging hierarchy of interactions for water in proteins (and, perhaps, for polymers in general), listed as follows in order of decreasing strength: ion-ion > water-ion > water-polar = polar-polar = water-water > water-hydrophobic. There is clear evidence of specific interactions in synthetic polymers in the form of hydrogen bonding of water to amide units in nylon-66,⁶ at ester or carboxyl sites in amorphous acrylic polymers,¹ at OSO_3Na groups in sodium cellulose sulfate,⁷ at polar groups in epoxy resins,^{8,9} and in ion clusters in perfluorinated sulfonate membranes.¹⁰

Interpretation of data from hydrated polymers is impaired by numerous complicating factors: typically, water may act as a plasticizer or antiplasticizer depending on concentration and temperature,⁵ the structural organization of absorbed water is sensitive to polymer mobility,¹ polymer conformational changes can accompany hydration, the presence of a third component such as a salt can alter the way in which water behaves,² effects of cross-linking can be significant, and water is affected by both equilibrium and nonequilibrium factors, the latter displaying strong temperature and concentration dependence.¹¹ Hysteresis effects are often observed on heating and cooling, and, more generally, events in one temperature

regime need not extrapolate in an obvious way to another regime.

Many of the earlier studies sought to determine the nature and amount of different water types in the polymer, described variously as "bound" and "free", "freezable" and "nonfreezable", and "associated" water. More refined studies have detected as many as four distinguishably different types of water ranging from the most tightly bound to free, bulklike water.¹² Thermodynamic measurements¹³ demonstrate the stepwise character of the hydration process in water/protein systems.

Studies to date reveal that estimates of the relative proportions of different water types can depend sensitively on the technique used² and, as a consequence of the hysteresis effects alluded to earlier, on the thermal cycling of the sample. Calorimetric methods such as differential scanning calorimetry (DSC)¹ monitor the gross phase changes of water in polymers. Such thermodynamic measurements permit the characterization of hydrated systems without recourse to detailed molecular models. On the debit side, parameters such as the enthalpy of fusion are insensitive to water below a certain concentration and, as such, serve only to provide an estimate, under certain assumptions, of the amount of freezable water in the polymer. Water remains unseen in the DSC experiment either because the *change* in heat capacity associated with highly dispersed water is too small to be detected or because the amount of water involved is too small to fall within the range of sensitivity of the equipment or both. The latter difficulty may be obviated by recording DSC thermograms as a function of water content as described later. Nuclear magnetic resonance (NMR), on the other hand, can probe the behavior of water even at concentrations within the so-called bound water regime and can both qualitatively and quantitatively distinguish between water that retains mobility to quite low temperatures and more normal water that freezes in the vicinity of 273 K. It has been recognized that water in a number of polymer systems behaves in a glasslike fashion with a glass transition temperature, T_g , that is far below 273 K.^{10,14,15}

In this paper we seek a clearer understanding of some of the more puzzling aspects of water in polymers using, in consort, the techniques of NMR and DSC. Studies on the copolymer poly(*N*-vinyl-2-pyrrolidone/methyl methacrylate), P(NVP/MMA), principally exploit the characteristic sensitivity of NMR to the bound phase in order

to delineate quantitatively bound and free (or nearly free) water. These data are then compared with DSC results on the same range of samples for which the degree of hydration is the disposable parameter.

Part 2 of this overall study, the following paper in this issue, describes a parallel set of experiments on hydrated PHEMA, a system demonstrably different in character than hydrated P(NVP/MMA). A comparison of the two sets of results provides interesting further insight into the subtleties of water behavior in the systems under consideration.

Experimental Section

NMR Measurements. Proton resonances were recorded on a Bruker SXP pulsed NMR spectrometer operating at 40 MHz and interfaced to a Commodore PET computer via a Biomation transient recorder. Spin-lattice (T_1) and rotating frame ($T_{1\rho}$) relaxation times were derived from the 180° - τ - 90° ¹⁶ and 90° - 90° phase shift spin-locking¹⁷ sequences, respectively. Short, intermediate, and long spin-spin (T_2) relaxation decays utilized the 90° - τ - 90° solid echo,¹⁸ the 90° pulse, and the 90° - τ - 180° and CPMG spin-echo sequences.¹⁸ Sample temperature was controlled to ± 1 K, and specific details of data analysis are reported elsewhere.¹⁹ Because of hysteresis effects, it is important to specify the temperature cycles used, and, unless otherwise indicated, NMR data were recorded initially as a function of decreasing temperature from ambient temperature to 150 K. On completion of the low-temperature run data were then recorded at progressively higher temperatures above room temperature.

DSC Measurements. Measurements were performed on a Perkin-Elmer DSC-4 differential scanning calorimeter interfaced to a thermal analysis data system. Thermograms were recorded at least twice to ensure reproducibility in the recorded data. Energy and temperature calibration relied on the fusion peak of indium as a reference. Sample weights, typically of the order of 5 mg, were determined to an accuracy of ± 0.01 mg on a Sartorius balance. Reducing the scanning rate from 20 to 5 K min⁻¹ produced no significant change in the recorded thermograms.

Sample Materials. The random copolymer under investigation, available commercially as Lidofilcon, contained 70.66 wt % *N*-vinyl-2-pyrrolidone, 29.12 wt % methyl methacrylate, 0.026 wt % ethylene glycol dimethacrylate, 0.19 wt % allyl methacrylate, and 0.10 wt % 2,2-azobis(isobutyronitrile). As pointed out by Ratner and Miller,²⁰ the presence of the MMA units in the copolymer binds the water-soluble NVP chains together by a hydrophobic mechanism. The cross-linked homopolymer of poly(vinylpyrrolidone) (PNVP) was obtained from Aldrich Chemicals. Hydration of the copolymer was achieved by soaking the dry film of thickness 0.30 ± 0.02 mm in distilled water for 24 h. For the saturated sample, excess surface water was removed by pressing the sample film gently between sheets of absorbent paper before transfer to a stoppered NMR tube or DSC sample pan as the case may be. Samples with lower water contents were cut from the film after progressively longer drying periods. The actual water content was determined from the weight lost after heating the sample at 420 K for at least 14 h. Samples are designated S(W), where W is the wt % water content relative to the 100 wt % dry material S(0). In one series of experiments, replacement of H₂O by D₂O is denoted by the subscript D in the sample nomenclature. Prior to soaking in D₂O, the deuteriated samples were washed in D₂O and dried repeatedly to remove any water in the material as received.

Results and Discussion

NMR Data. A prerequisite examination of the dry copolymer S(0) was carried out to facilitate subsequent interpretation of the hydrated system. NMR T_1 , $T_{1\rho}$, and T_2 data are presented as a function of temperature in Figure 1 along with the response for neat PNVP and PMMA. The various relaxation processes in PMMA are well established.^{21,22} From the homopolymer data it is clear that α -CH₃ motion (designated C on the diagram) is a major source of T_1 relaxation around 273 K and $T_{1\rho}$ relaxation at ~ 170 K. Between 270 and 390 K, $T_{1\rho}$ for the

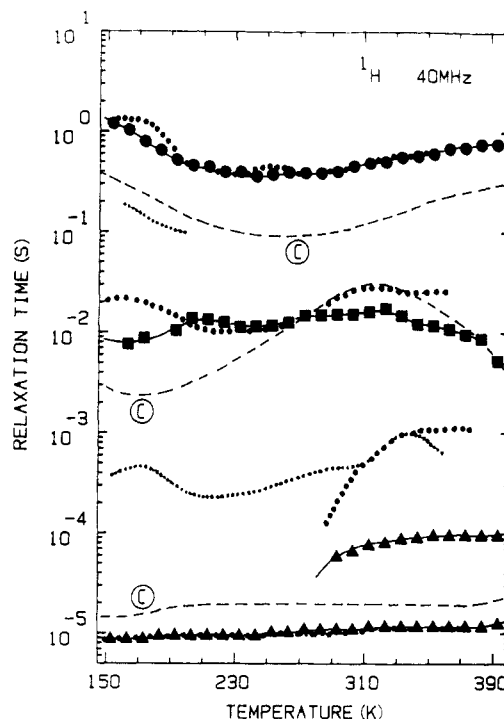


Figure 1. Proton T_1 (●), $T_{1\rho}$ (■), and T_2 (▲) data for dry P-(NVP/MMA). The short and long T_2 components are denoted, respectively, T_{2S} and T_{2L} in the text. Data for PMMA (---) and PNVP (····) are included for comparison. The more closely spaced dots in the PNVP data represent the shorter component. $I(T_{2L}) \sim 0.1$ for P(NVP/MMA). α -CH₃ relaxation in PMMA is denoted by C (see text).

copolymer is shorter than $T_{1\rho}$ for either of the two homopolymers, perhaps reflecting a higher degree of NVP cross-linking in the homopolymer relative to the copolymer. The long, T_{2L} , component of $\sim 10\%$ intensity in the copolymer has its analogue in PNVP and may be due to residual monomer or trace amounts of water in the nominally dry copolymer sample. The modest increase in the short, T_{2S} , component over the temperature range studied shows that general polymer motions do not set in below 390 K, which is the upper limit of our measurements.

It is instructive to examine quantitatively those temperature regions where relaxation via α -CH₃ motion is most efficient. On the assumption that this is the dominant source of relaxation and that a common spin temperature is established throughout the copolymer, the observed relaxation rate k ($=T_1^{-1}$ or $T_{1\rho}^{-1}$) is

$$k = (N_m/N_T)k_1^\circ \quad (1)$$

where k_1° is the intrinsic relaxation rate for a methyl proton, N_m is the number of methyl protons, and N_T is the total number of protons in the copolymer. Equation 1 may be written in terms of the mass fraction, w_1 , of MMA as follows

$$(8.11 - 0.11w_1)k = 3w_1k_1^\circ \quad (2)$$

k_1° may be estimated from the magnitude of the minimum (100 ms) at 273 K in neat PMMA. In this case $k = 3k_1^\circ/8 = (100 \text{ ms})^{-1}$, and therefore $k_1^\circ = 26.7 \text{ s}^{-1}$. The corresponding intrinsic rate of methyl proton relaxation in the rotating frame (at 170 K) is 1110 s^{-1} . Substituting these values into eq 2 and noting that $w_1 = 0.29$ reveal that the predicted magnitudes of T_1 and $T_{1\rho}$ minima for the copolymer are, respectively, 350 and 8.4 ms, which compare favorably with the observed magnitudes in S(0) of 360 and 7.5 ms. Thus the assumption that the α -CH₃ groups in MMA are the principal source of relaxation at the tem-

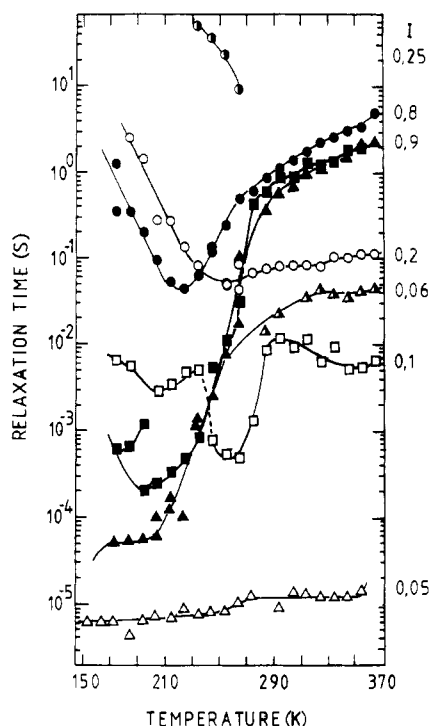


Figure 2. Proton T_1 (○, ●, ○), T_{1p} (□, ■), and T_2 (△, ▲, △) data for saturated P(NVP/MMA), S(345). The filled data points reflect glasslike water behavior (see text). Component intensities, I , in the high-temperature regime are indicated on the right-hand side of the diagram. $I = 0.25$ at the top of the diagram refers to T_1 (○).

peratures indicated is borne out. It also follows from the T_{1p} data that protons in NVP are within a distance of about 1.2 nm of a MMA methyl group.²³

NMR data for the saturated sample S(345) reflect the combined response for water and host polymer (Figure 2). However, as elegantly demonstrated in earlier studies,²⁴⁻²⁶ the situation is not a simple superposition of the individual behavior of water and polymer. Apart from obvious interactive effects such as plasticization, cross-relaxation can alter appreciably the NMR response of the system and lead to further interpretive sophistication. Briefly, cross-relaxation involves three steps:²⁴ The transfer of spin energy between different types of water by means of chemical exchange is the first step. If the rate of exchange is rapid, averaged single-component relaxation times are predicted.²⁷ Resing and co-workers²⁸ have also shown that chemical exchange is responsible for the creation of minima (or plateaus) in the water T_2 as the temperature is increased. Second, the transfer of magnetization throughout the proton spin system of the polymer by spin diffusion as discussed above. The third step is the transfer of spin energy across the water/polymer phase boundary by a mechanism of mutual spin flips between bound water and polymer surface protons. Taken with the first and second steps, this mode of relaxation can contribute significantly to the observed spin-lattice relaxation. A preliminary examination of S(345) using the Edzes-Samulski procedure²⁴ confirmed that cross-relaxation effects were negligible at room temperature.

We shall approach the interpretation of data in Figure 2 by examining, in parallel, the sample $S_D(355)$ saturated with D_2O (Figure 3). Consider first the $S_D(355)$ results below 273 K, where the dominant T_{1L} component ($I = 0.8-0.9$) closely mimics T_1 for the dry polymer. Assignment of T_{1S} to small amounts of unexchanged H_2O in the sample is supported by the appearance of long T_1 and T_2 components ($I \sim 0.07$) above 273 K. T_{1p} minima at ~ 170 and

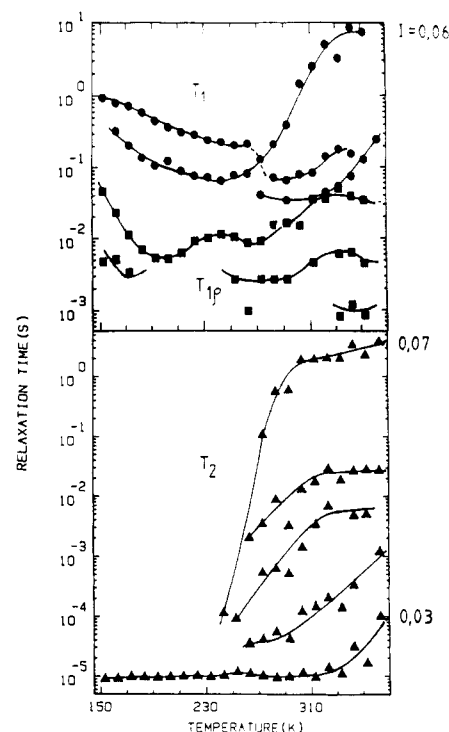


Figure 3. Proton T_1 (●), T_{1p} (■), and T_2 (▲) data for sample $S_D(355)$ saturated with D_2O . Selected component intensities in the high-temperature regime are as indicated.

~ 200 K are assigned respectively to the motion of $\alpha-CH_3$ and to bound water; this latter assignment will be discussed further in due course. Because of the small amount of bound water present, the corresponding mobile T_2 component is not resolved until it attains a magnitude of $\sim 10^{-4}$ s, at 240 K. The single T_2 below 240 K is comparable in magnitude to T_2 for the nominally dry sample (Figure 1) which may, as noted earlier, contain a similar amount of residual H_2O .

The data for $S_D(355)$ above 273 K are complex. The long T_1 is the residual H_2O signal whereas the intermediate and short T_1 components are ascribed to polymer. The fact that these T_1 components are appreciably shorter than T_1 for the nominally dry sample implies that the polymer is plasticized by the D_2O . The presence of D_2O also permits resolution of up to three T_{1p} components in $S_D(355)$ compared to the single T_{1p} in $S(0)$, indicating a broad distribution of cooperative motions and, perhaps, preferential plasticization of one part of the copolymer over another. The broad T_{1S} minimum above room temperature and T_{1p} minima at ~ 265 and ~ 350 K also appear in the $S(345)$ data. Their assignment to specific molecular motions will be addressed later in the discussion.

Resolution of the T_2 decay into several components does not necessarily imply multiple discrete phases in the sample but may reflect the combined effects of a broad distribution of motional correlation times and chemical exchange.²⁹ It is beyond doubt that at least two-thirds of the polymer prematurely attains a mobility far in excess of that achieved at comparable temperatures in the dry material, again strongly supporting the view that D_2O plasticizes the polymer. Note, too, that this mobility sets in at temperatures below 273 K from which it would appear that supercooled D_2O can assume the role of plasticizer.

Reverting to the $S(345)$ results (Figure 2), the appearance of minima in T_1 and T_{1p} at 230 K and 180 and 200 K, respectively, together with the long, T_{2L} , component beginning at ~ 170 K is characteristic of the glasslike re-

sponse of water observed earlier in a range of hydrated polymer systems.^{10,14,15,30} Comparison of T_1 data for the macromolecular phase in the D_2O - and H_2O -saturated samples suggests that cross-relaxation is significant at low temperatures. The relaxation-temperature profiles (filled data points in Figure 2) follow the response expected of a mobile liquid at high temperatures where T_1 , $T_{1\rho}$, and T_2 converge and where component intensities more or less approach the known fraction (0.83) of water protons in S(345). It is clear that above room temperature there is only water averaged over all environments which is essentially bulklike and includes "associated" water characterized by a correlation time τ_c , somewhat longer than τ_c for pure water.³¹ The plateau in T_{2L} between 170 and 210 K together with the two associated $T_{1\rho}$ minima may well indicate at least two distinguishably different types of bound water having different T_g values and/or energies of activation. This is consistent with the heterogeneous character of water sites in hydrated polymers. The long T_1 component between 230 and 270 K ($I \approx 0.25$) is attributed to ice in the polymer.

T_{1S} above room temperature with an intensity of ~ 0.2 is of comparable magnitude to the short and intermediate T_1 components in $S_D(355)$ and is again assigned to plasticized polymer. The $T_{1\rho}$ polymer minimum at 200 K (open squares in Figure 2) is coincident with the principal water minimum and manifests the effects of cross-relaxation. The α -CH₃ relaxation minimum is anticipated at a somewhat lower temperature, as in Figure 1. The $T_{1\rho}$ minimum at ~ 260 K and the associated increase in T_{2S} signify the onset of polymer plasticization whereas the $T_{1\rho}$ minimum at ~ 350 K is tentatively assigned to the onset of general motions, coincident with the disappearance of the albeit exceedingly weak ($I = 0.05$) polymer T_{2S} component. These motional assignments have their analogues in the $S_D(355)$ data, consideration of which was deferred until now. The intermediate T_{2i} ($I = 0.06$) represents water of intermediate mobility plus polymer that has been plasticized at much lower temperatures; it is noteworthy that T_{2i} appears at about the same temperature where a mobile proton T_2 signal is first observed in $S_D(355)$. Consideration of the component T_2 intensities indicates that about 6% of the polymer contributes to the longest T_2 component.

To summarize thus far, it is clear that a significant part of the water in S(345) is bound in the sense that it attains mobility of appreciable proportions at 170 K, that all the water is bulklike in the high-temperature regime, and that some two-thirds of the water-saturated polymer is plasticized at room temperature and above.

Having established the role of water at the two extremes of hydration, attention is now directed to the way in which T_2 behaves as a function of water content (Figure 4). In anticipation of subsequent comparisons with DSC results, these data were recorded as a function of increasing temperature beginning at 150 K. There are a number of interesting features: (i) The long, T_{2L} , component clearly monitors water behavior with, perhaps, a modest contribution from plasticized polymer above room temperature. The extent to which plasticization occurs will be sensitive to the degree of cross-linking in the copolymer. (ii) There is a tendency for T_{2L} to appear at a marginally lower temperature in the more heavily hydrated samples, implying a similar temperature dependence for T_g . (iii) T_{2L} undergoes a smooth transition through 273 K, but the gradient of T_{2L} vs temperature becomes steeper with increasing water content as 273 K is approached. (iv) The magnitude of T_{2L} tends to decrease as the water content

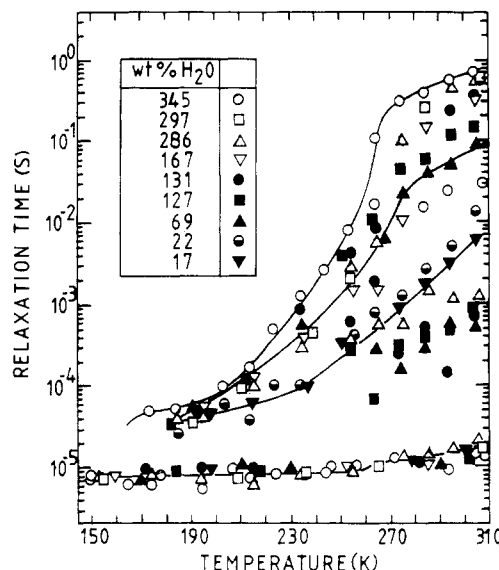


Figure 4. Representative T_2 data for hydrated P(NVP/MMA) for different water contents recorded as a function of increasing temperature.

is lowered. (v) The resolution of a second component of intermediate mobility, T_{2i} , is possible in all cases except S(22) and S(17). (vi) The magnitude of the short, T_{2S} , component is not particularly sensitive to water concentration. The modest increase at ~ 250 K at the higher water concentrations coincides with the onset of plasticization as discussed earlier.

The overall dependence of T_2 on water content generally complies with the notion of heterogeneous water sites in the sense of diverse environments or, indeed, diverse averages for a given environment. A precise demarcation of uniquely characteristic sites in hydrated polymers through interpretation of NMR relaxation data is impaired by the approximations inherent in the signal decomposition procedure for a distribution of proton environments which includes the effects of chemical exchange. Generally, however, as the water content decreases there is a preferential decrease in the amount of free, or nearly free, water, and the distribution is biased toward the more tightly bound states characterized by a lower T_{2L} . Undoubtedly, too, plasticized polymer contributes significantly to T_{2i} and much less so to T_{2L} in the more heavily hydrated material above room temperature. In this sense, the NMR data support the concept of a range of physical environments in the polymer such as those associated with hydrophilic moieties or porous regions, as alluded to in the Introduction, where water behavior differs appreciably from the bulk. Quantification of these ideas requires consideration of the corresponding component intensities which, as it turns out, are particularly revealing.

The T_2 component intensity data in Figure 5 more clearly differentiate between the principal types of water in P(NVP/MMA). Referring first to the results for S(17), it is observed that nonfreezable water becomes mobile above 190 K, achieving a temperature-independent intensity $I_L = 0.22$ which is systematically higher but, within experimental error, equal to the calculated fraction of water protons in the sample denoted by the dashed lines in Figure 5. Note that I_L does not increase near 273 K as would be expected from the melting of bulklike water if present. Therefore, within the sensitivity of NMR, all the water in S(17) is nonfreezable. S(22) behaves in similar fashion. For S(69) through S(345), I_L becomes progressively more intense in the vicinity of 273 K, manifesting increasing amounts of melting, bulklike water. The

Table I
Pertinent T_2 Intensity Data for P(NVP/MMA) Taken from Figure 5

sample	I_{WP}^a	experimental intensities ^b				relative amounts of each component ^c		
		I_{L1}	I_{L2}	I_{L3}	I_{L4}	I_{L1}/I_{WP}	I_{L2}/I_{WP}	I_{L3}/I_{WP}
S(345)	0.83	0.20	0.14	0.05	0.88	0.24 (83)	0.17 (58)	0.06 (21)
S(286)	0.80	0.21	0.12	0.12	0.83	0.26 (74)	0.15 (43)	0.15 (43)
S(131)	0.64	0.38	0.20	0.18	0.70	0.59 (78)	0.31 (41)	0.28 (37)
S(69)	0.49	0.48	0.42	0.08	0.57	0.98 (68)	0.86 (59)	0.16 (11)
S(22)	0.23	0.26	0.26	0	0.26	1.00 (22)	1.00 (22)	0 (0)
S(17)	0.19	0.22	0.22	0	0.26	1.00 (17)	1.00 (17)	0 (0)

^a Fraction of water protons. ^b $I_{L1} - I_{L4}$ are defined in the text. Recall that plasticized polymer contributes to I_{L3} . ^c For S(22) and S(17), I_{L1}/I_{WP} and I_{L2}/I_{WP} are set equal to 1. The numbers in parentheses denote the corresponding weight percentages relative to the dry polymer.

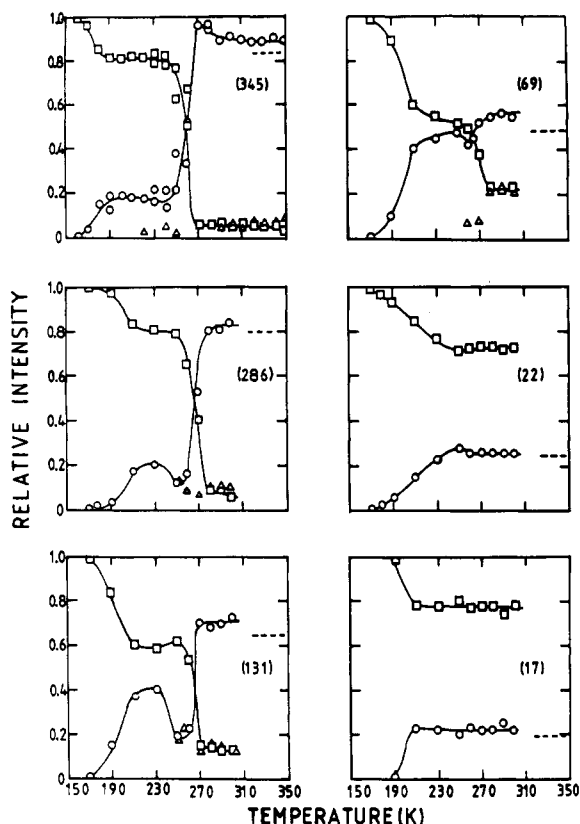


Figure 5. Component T_2 intensity data for samples of different water contents: T_{2L} (○), T_{2i} (△), and T_{2a} (□). The dashed lines denote the calculated water proton fractions.

presence of bulklike water in samples with high water content is also inferred from their translucent appearance following immersion in liquid nitrogen. Samples containing only bound water retain their transparency under similar conditions.

The observation that the high-temperature plateau in I_L tends to be systematically higher than the calculated total fraction of water protons may be explained in a number of ways: First, there is a tendency systematically to overestimate the intensity of T_{2L} in the decomposition procedure.³² Second, some of the water may have been driven off during the NMR experiment, resulting in an underestimation of the water content and therefore of the calculated fraction of water protons in the sample. Third, as suggested above, part of the polymer may be plasticized to such a degree that it contributes directly to T_{2L} . It is recalled that about 60% of the polymer in S_D(355) achieves a mobility commensurate with T_{2i} and T_{2L} above room temperature. It is probable that all three contribute to the observed discrepancies, although one would expect that proportionately less water would be driven off in samples of lower water content.

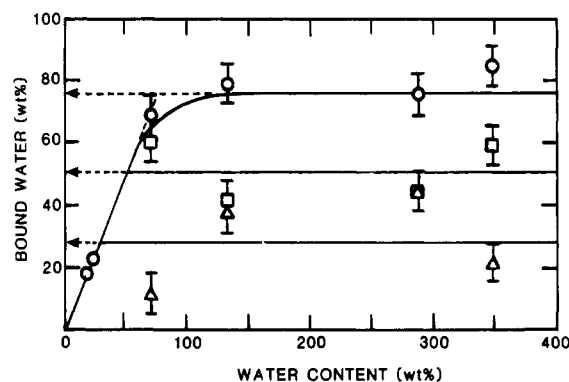


Figure 6. Plots of the nonfreezable bound water fraction I_{L1}/I_{L4} (○) and the resolved mobile components at 250 K, I_{L2}/I_{L4} (□) and I_{L3}/I_{L4} (△), as a function of water content. The data are taken from Table I.

The decrease in I_L between 230 and 270 K for samples which contain bulklike water is significant. Note that there is no concomitant rise in I_S as would be the case if some of the water rendered mobile at lower temperatures began to freeze again. Rather, the observed decrease in I_L accompanies the resolution of a third, intermediate (T_{2i}) component (Figure 4). The overshoot in I_L just above 273 K in S(345) reflects an inability to resolve T_{2i} and T_{2L} at these temperatures.

Analysis of the data focuses upon three intensity regimes: the peak value of I_L near 230 K denoted I_{L1} , which monitors the maximum amount of the nonfreezable water phase; the values of I_L and I_i at the minimum in the I_L -temperature curves near 250 K, denoted respectively I_{L2} and I_{L3} , which quantify the relative amounts of the two distinguishably different mobile phases described by T_{2L} and T_{2i} , respectively; and the magnitude I_{L4} of the high-temperature I_L plateau, which gives a measure of the total water present plus a possible contribution from highly plasticized polymer. In the absence of precise information, the theoretical estimate of the total water, denoted I_{WP} , is used to compute the relative amounts of different phases present. The various data listed in Table I and pertinent results plotted in Figure 6 will be discussed along with the DSC data reported in the next section of the paper.

DSC Data. Figure 7 portrays a typical set of endotherms for samples of different water concentrations heated at a rate of 5 K min⁻¹ from 200 to 300 K. The principal features, which are in accord with earlier observations on hydrated polymers,^{1-3,10-15,33} include (i) the absence of peaks below a certain water concentration, indicating that the amount of freezable water detected by DSC is less than the total water content of the sample; (ii) the appearance of a structure on the endothermic peaks that has been ascribed to a distribution of melting points in the sample;^{1,2} and (iii) the fact that the peak area spans a temperature range of only 250–276 K, indicating that DSC is insensitive

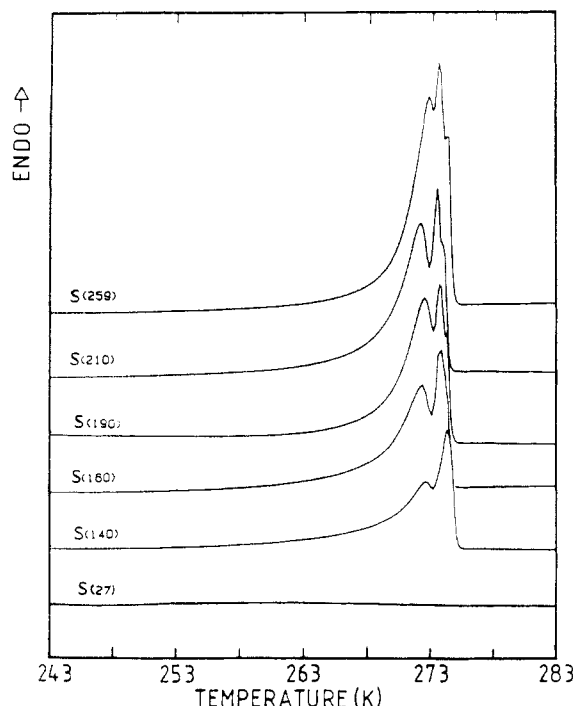


Figure 7. Typical DSC endotherms for hydrated P(NVP/MMA) as a function of water content. The samples were heated at a rate of 5 K min⁻¹.

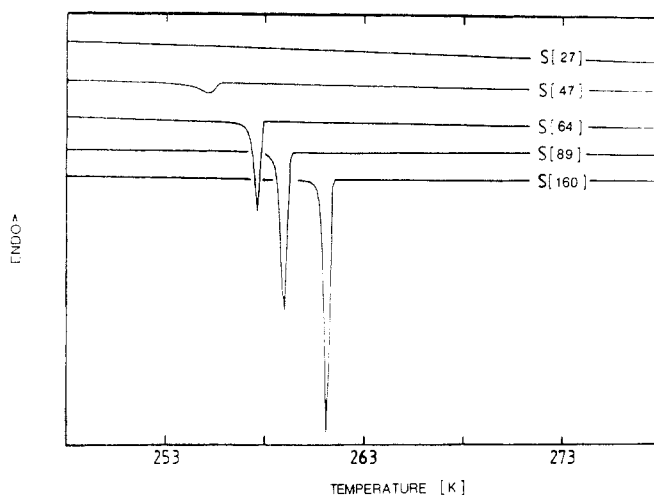


Figure 8. DSC exotherms for hydrated P(NVP/MMA) as a function of water content. The samples were cooled at a rate of 5 K min⁻¹.

to events below 250 K. Note that the area under the peak denotes the change in enthalpy associated with the thermal event under consideration, in this case, the melting of freezable water.

Exothermic data recorded as a function of cooling are reported in Figure 8. In this case the exothermic troughs are much sharper; they correspond to much smaller changes in enthalpy and reflect appreciable supercooling, of the order of $\Delta T_m \approx 14$ –21 K depending on water concentration. The differences in peak temperatures on heating and cooling are manifestations of the general hysteresis observed in a wide range of experimental data.^{2,34,35}

Heretofore, the nonfreezable water content has either been equated with the maximum amount of water for which no enthalpic peak has been detected or it has been estimated as the difference between the total water content, determined gravimetrically, and the amount of freezable water computed from the peak area by using the

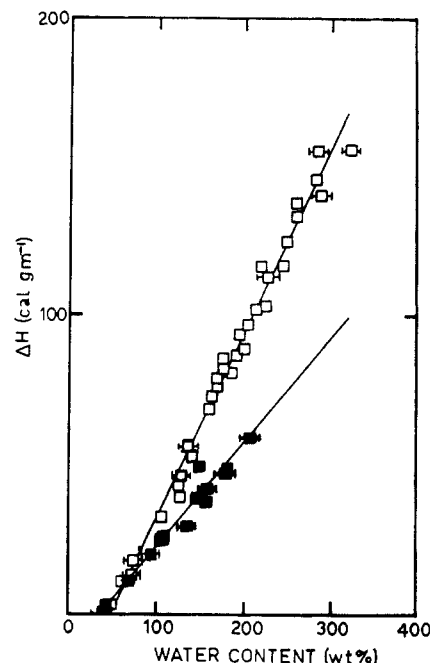


Figure 9. Change in enthalpy, ΔH , versus water content, W , for endothermic (\square) and exothermic (\blacksquare) DSC data. Regression procedures have been used to fit the data as follows: (\square) $\Delta H = 0.61W - 28.69$ ($R = 0.99$); (\blacksquare) $\Delta H = 0.34W - 12.63$ ($R = 0.99$).

heat of fusion for bulk water, $\Delta H_{fus} = 79.6$ cal g⁻¹.³⁶ The latter method is clearly incorrect since the heat of fusion of freezable water is not constant;² $\Delta H_{fus} = 79.6$ cal g⁻¹ is an upper limit that inevitably leads to an overestimation of the amount of nonfreezable water in the hydrated system.

Adopting the first procedure, the integrated change in enthalpy (per gram of dry polymer) is recorded as a function of water content in Figure 9 for the heating and cooling cycles. The linear fit to the endothermic data yields a differential heat of fusion $\Delta H_{fus} = 61 \pm 5$ cal g⁻¹ for the freezable water and a value of 47 ± 7 wt % for the maximum amount of nonfreezable water that the polymer can support. The corresponding results for the exothermic data are, respectively, 34 ± 5 cal g⁻¹ and 37 ± 7 wt%. The differences in the two estimates of nonfreezable water may or may not be significant, but it could be argued that supercooling terminates in *rapid* nucleation, inducing a greater change in heat capacity (to which DSC is sensitive) and therefore the detection of a greater amount of freezable water. Ladbroke and co-workers³³ were concerned that the determination of differential heats of fusion in this way ignored the possibility that the amount of nonfreezable water, coexisting with freezable water, might vary with total water content. These fears would appear to be unwarranted within the accuracy of the data in Figure 6. Pouchly and co-workers¹¹ also remind us that the area under the endothermic peaks represents the heat of melting, not of ice into pure water, but of the heat associated with the transformation of ice into water in the mixed phase. The two situations differ by the heat of mixing of water with polymer, which, they argue, is probably negative. A low heat of fusion and a correspondingly low freezing point imply a much more dispersed water phase.² The lower differential heat of fusion associated with the cooling cycle data is consistent with the observation of a significantly depressed freezing point ($\Delta T_m \approx 14$ –21 K).²

The insensitivity of DSC to events below 250 K and to the thermal processes associated with the onset of mobility

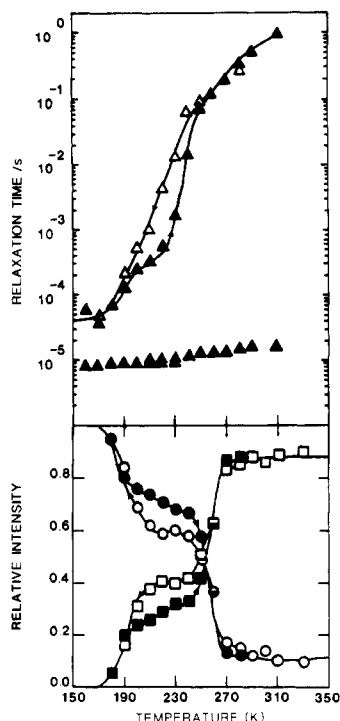


Figure 10. T_2 data for S(260) recorded under heating and cooling cycles. The filled data points denote the heating cycle and the unfilled points the cooling cycle (see text).

in the bound water fraction is rationalized by Pouchly and co-workers¹¹ as follows. At low temperatures, where a significant proportion of the water is immobile, water-rich samples behave in similar fashion to those with initially lower water contents, and, as such, the phase transformation below 250 K does not proceed in accordance with equilibrium predictions. As alluded to in the introductory section of the paper, they conclude generally that the fraction of nonfreezing water is determined by a number of equilibrium and nonequilibrium factors, the latter being strongly temperature and concentration dependent. More specifically, at water concentrations within the bound water regime and/or at temperatures below 250 K, the solidification of water is hampered by kinetic factors arising from reduced water diffusivity and constraints imposed by the rigid polymer network.

Intercomparison of NMR and DSC Results. The marked hysteresis in DSC data prompts an examination of similar effects in the NMR response, as observed in other hydrated systems.³⁵ Hysteresis is most prominent in samples of intermediate hydration as shown for S(260) in Figure 10, where data were first recorded as a function of increasing temperature and subsequently as a function of decreasing temperature. In this case it was not possible to resolve three T_2 components due to limitations of the decomposition procedure where resolution of multicomponent T_2 's depends invidiously on a favorable combination of relative magnitudes and intensities. Note that the change in I_L between 253 and 273 K (the temperature range within which DSC effects are detected) is greater on heating than on cooling and that T_{2L} is longer for the cooling cycle. Both these observations imply more mobile water, and almost certainly plasticized polymer, at a given temperature during cooling. This is consistent with supercooling and the observation of a lower enthalpy of fusion upon cooling. The fact that the T_2 data could not be resolved into three components renders further comparisons with DSC data difficult.

In an earlier NMR study, Katayama and Fujiwara³⁵ discussed the hysteresis behavior of water in polyacryl-

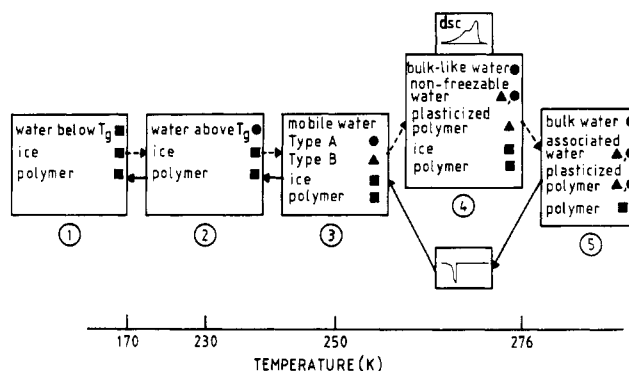


Figure 11. Specification of five thermal equilibrium states in hydrated P(NVP/MMA). The dashed and solid arrows denote, respectively, increasing and decreasing temperature cycles. The symbols denote the T_2 associated with each component as follows: T_{2S} (■), T_{2i} (▲), T_{2L} (●) (see text).

amide gels in terms of four thermal equilibrium states. The collated NMR and DSC data for P(NVP/MMA) suggest five such states as portrayed in Figure 11. State 1 prevails at temperatures below ≈ 170 K and comprises rigid polymer, ice, and glasslike water below its glass transition temperature, T_g . At temperatures in excess of T_g the glasslike or bound water achieves appreciable mobility as reflected in the NMR data. The fraction of this mobile component attains a maximum value of 76 ± 10 wt % at ≈ 230 K (state 2). In keeping with the earlier interpretation of the low-temperature plateau in T_{2L} for S(345), two bound or nonfreezable water components characterized by long (type A) and intermediate (type B) T_2 components are resolved at 250 K with respective intensities of 50 ± 10 and 28 ± 15 wt % (state 3). This temperature also heralds the onset of plasticization, as demonstrated in Figure 3, and plasticized polymer also contributes to the type B signal. Between 250 and 276 K, both DSC and NMR point to the coexistence of bulklike water, nonfreezable water, ice, plasticized polymer, and nonplasticized polymer (phase 4). Immediately above 276 K phase 5 comprises water averaged over all environments and includes bulk water, associated water, plasticized polymer, and nonplasticized polymer.

Examining the situation quantitatively, it is recalled from the NMR data recorded as a function of increasing temperature (Figure 5) that all but 50 ± 10 wt % of bulklike water, denoted type A and characterized by T_{2L} , freezes between 276 and 250 K. This estimate agrees remarkably well with the nonfreezable water fraction, 47 ± 7 wt %, predicted from the endothermic DSC results. The extent to which the two estimates are in accord is fortuitous in light of the associated experimental errors. The insensitivity of DSC to the more dispersed type B water of intermediate mobility plus plasticized polymer, characterized by T_{2i} , is evident. The fact that T_{2i} and T_{2L} are unresolved at lower temperatures and the neglect of plasticization effects accounts in part for earlier discrepancies between NMR and DSC estimates of the nonfreezable water fraction. DSC detects type A but not type B; NMR detects both.

Water contributing to the type B signal in all probability denotes bound water at specific polymer sites such as carbonyl groups. The more loosely bound type A water includes water that is more moderately influenced by the polymer matrix, for example, multilayer water and water in interstices. Energetically the differences in the two types of water are not all that different. Unfrozen water in proteins experiences a chemical shift of 1 ppm upfield of bulk water at the same temperature, indicating roughly

comparable but slightly weaker hydrogen bonding near the protein surface.² Similar conclusions are drawn from IR measurements. It has also been deduced that the binding of water directly onto the surface of poly[2-(2-hydroxyethoxy)ethyl methacrylate] is not much stronger than the average mutual interaction between water molecules in the bulk.¹¹ A lack of information on the precise contribution of plasticized polymer to the type B signal precludes quantification of the number of water molecules per NVP or MMA unit.

In conclusion, comparison of DSC and NMR data provides interesting insight into the role of water in a range of hydrated P(NVP/MMA) samples. Three types of water are detected: tightly bound (type B), more loosely bound (type A), and bulk water. Both type A and type B water are nonfreezable in the accepted sense of the term but undergo glasslike transitions at 170–200 K. NMR is sensitive to both type A and type B water whereas DSC is sensitive only to type A. A scheme drawn up in terms of five thermodynamic equilibrium states facilitates the intercomparison of NMR and DSC data and clarifies the hysteresis effects observed in hydrated P(NVP/MMA).

Acknowledgment. It is a pleasure to acknowledge useful discussions with research personnel at Bausch and Lomb in Rochester, NY, and in Waterford, Ireland. This research was supported jointly by Bausch and Lomb and the Industrial Development Authority of Ireland.

Registry No. Lidofilcon, 56551-60-1; water, 7732-18-5.

References and Notes

- (1) Rowland, S. P., Ed. *Water in Polymers*; ACS Symposium Series 127; American Chemical Society: Washington, DC, 1980.
- (2) Kuntz, I. D.; Kauzmann, W. *Adv. Protein Chem.* **1974**, *28*, 239.
- (3) McBrierty, V. J.; Douglass, D. C. *Phys. Rep.* **1980**, *63*, 61.
- (4) Stillinger, F. H. In Reference 1, p 11.
- (5) McCall, D. W. *NBS Spec. Publ. (U.S.)* **1969**, No. 331, 475. See also: Rowland, S. P.; Kuntz, I. L. In Reference 1, p 1.
- (6) Puffr, R.; Sebens, J. J. *Polym. Sci., Part C* **1967**, *16*, 79.
- (7) Hatakeyama, T.; Yoshida, H.; Hatakeyama, H. *Polymer* **1987**, *28*, 1282.
- (8) Moy, P.; Karasz, E. E. *Polym. Eng. Sci.* **1980**, *20*, 4.
- (9) Jelinski, L. W.; Dumais, J. J.; Stark, R. E.; Ellis, T. S.; Karasz, F. E. *Macromolecules* **1983**, *16*, 1021.
- (10) Pineri, M.; Eisenberg, A., Eds. *Structure and Properties of Ionomers*; NATO ASI Series C; Reidel: 1987; Vol. 198.
- (11) Pouchly, J.; Biros, J.; Benes, S. *Makromol. Chem.* **1979**, *180*, 745.
- (12) Haly, A. R.; Snaith, J. W. *Biopolymers* **1971**, *10*, 1681.
- (13) Rupley, J. A.; Yang, P.-H.; Tollin, G. In Reference 1, p 111.
- (14) Boyle, N. G.; Coey, J. M. D.; McBrierty, V. J. *Chem. Phys. Lett.* **1982**, *86*, 3726.
- (15) McBrierty, V. J.; Smyth, G.; Douglass, D. C. In Reference 10, p 149.
- (16) Carr, H. W.; Purcell, E. M. *Phys. Rev.* **1954**, *94*, 630. Meiboom, S.; Gill, D. *Rev. Sci. Instrum.* **1958**, *29*, 688.
- (17) Hartmann, S. R.; Hahn, E. L. *Phys. Rev.* **1962**, *128*, 2042.
- (18) Powles, J. G.; Mansfield, P. *Phys. Lett.* **1962**, *2*, 58.
- (19) McBrierty, V. J. *Polymer* **1974**, *15*, 503.
- (20) Ratner, B. D.; Miller, I. F. *J. Polym. Sci., Polym. Chem. Ed.* **1972**, *10*, 2425.
- (21) Douglass, D. C.; McBrierty, V. J. *Macromolecules* **1978**, *11*, 766.
- (22) Albert, B.; Jerome, R.; Teyssie, P.; Smyth, G.; Boyle, N. G.; McBrierty, V. J. *Macromolecules* **1985**, *18*, 388.
- (23) McBrierty, V. J.; Douglass, D. C. *Macromol. Rev.* **1981**, *16*, 295.
- (24) Edzes, H. T.; Samulski, E. T. *Magn. Reson.* **1978**, *31*, 207.
- (25) Chang, D. C.; Woessner, D. E. *Science (Washington, D.C.)* **1977**, *198*, 1180.
- (26) Resing, H. A.; Foster, K. R.; Garroway, A. N. *Science (Washington, D.C.)* **1977**, *198*, 1181.
- (27) Zimmerman, J. R.; Brittin, W. E. *J. Phys. Chem.* **1957**, *61*, 1328.
- (28) Resing, H. A. *Adv. Mol. Relax. Processes* **1972**, *3*, 199.
- (29) Hoeve, C. A. J. In Reference 1, p 135.
- (30) Boyle, N. G.; McBrierty, V. J.; Douglass, D. C. *Macromolecules* **1983**, *16*, 75.
- (31) See, for example: Wong, T. C.; Ang, T. T. *J. Phys. Chem.* **1985**, *89*, 4047.
- (32) Wardell, G. E.; McBrierty, V. J. *Proc. R. Ir. Acad., Sect. A* **1973**, *73*, 63.
- (33) Ladbrooke, B. D.; Jenkinson, T. J.; Kamat, V. B.; Chapman, D. *Biochim. Biophys. Acta* **1968**, *164*, 101.
- (34) Lee, H. B.; Jhon, M. S.; Andrade, J. D. *J. Colloid Interface Sci.* **1975**, *51*, 225.
- (35) Katayama, S.; Fujiwara, S. *J. Phys. Chem.* **1980**, *84*, 2320.
- (36) The units calories per gram have been retained to facilitate comparison with the significant body of comparable data in the literature.

Water in Hydrogels. 2. A Study of Water in Poly(hydroxyethyl methacrylate)

Gerard Smyth, Francis X. Quinn, and Vincent J. McBrierty*

Department of Pure and Applied Physics, Trinity College, Dublin 2, Ireland.

Received January 21, 1988; Revised Manuscript Received April 27, 1988

ABSTRACT: Collated broad-line NMR and DSC measurements sensitively probe the behavior of water in hydrated poly(hydroxyethyl methacrylate) (PHEMA). NMR reveals that bound water becomes mobile at ~180 K in keeping with observations in many other hydrated polymers; DSC is insensitive to events at these temperatures. In samples with a high water content, a fraction of this mobile water subsequently freezes between 230 and 260 K. The amount of freezable and nonfreezable water in hydrated PHEMA is determined quantitatively. Preliminary cross-relaxation experiments at 253 and 293 K indicate that NMR spin-lattice relaxation rates for water will be overestimated if the effects of cross-relaxation between the polymer and water proton spin systems are neglected. Although PHEMA is less hydrophilic than poly(*N*-vinyl-2-pyrrolidone/methyl methacrylate), studied in part 1, the relative fraction of bound water is significantly higher. Hysteresis effects in hydrated PHEMA are investigated in some detail.

Introduction

Part 1 of this study,¹ the preceding paper in this issue, briefly reviewed the general literature on hydrogels and examined specifically the role of water in poly(*N*-vinyl-2-pyrrolidone/methyl methacrylate) copolymer P(NVP/MMA). This paper reports on a second hydrogel, poly-

(hydroxyethyl methacrylate) (PHEMA), whose properties differ in a number of intriguing ways from those of P(NVP/MMA).

PHEMA has received wide attention primarily due to its biological compatibility.^{2–14} Swelling experiments¹⁰ indicate a secondary noncovalent structure superimposed